# SUSTAINABLE BIO-COMPOSITES BASED ON AMURA STARCH AND SUGARCANE BAGASSE: MECHANICAL, THERMAL, AND MOISTURE PERFORMANCE

**Abdulmalik, S.S.*, Muhammad, J.Y. and Bala, A.**

Department of Mechanical Engineering, Nigerian Army University Biu, P.M.M 1500, Borno State, Nigeria

*Corresponding email: alhajisani.sa@gmail.com

**ABSTRACT**

*Starch is particularly attractive due to its abundance, low cost, and inherent biodegradability. When processed with plasticizers into thermoplastic starch (TPS), starch can be melt processed similarly to conventional plastics, however, the challenge remains that TPS typically exhibits inferior mechanical strength, thermal stability, and moisture resistance compared to petrol-based polymers. In this study, bio-composites were produced using Tacca leontopetaloides (Amura) starch as a bio-polymer matrix, glycerol as a plasticizer, and sugarcane bagasse powder (BGP) as lignocellulosic reinforcement. Six formulations (0–2.5 wt% BGP with constant 5 mL glycerol) were synthesized and characterized for their structural, mechanical, thermal, and moisture-resistance properties. To Examined the composite; FTIR, XRD, TGA, tensile, hardness, and moisture absorption were used. Fourier Transform Infrared (FTIR) spectroscopy confirmed hydrogen bonding interactions between the hydroxyl groups of starch and cellulose, indicating strong interfacial adhesion. X-ray diffraction (XRD) revealed that bagasse incorporation induced partial crystallinity within the amorphous starch–glycerol matrix. The tensile strength increased with filler loading, peaking at 2 % BGP (≈ 2.5 MPa), accompanied by improved hardness (6.7 HV) and reduced ductility, signifying optimal reinforcement and uniform dispersion. Thermogravimetric analysis (TGA) and derivative thermogravimetry (DTG) demonstrated enhanced thermal stability and delayed onset of degradation with increasing BGP content. Moisture absorption declined to 11.85 % at 2.0 % BGP due to strong starch–cellulose hydrogen bonding, which limited water diffusion. The results indicate that the most optimal biocomposite, in terms of tensile, Moisture absorption and, thermal stability was achieved with 2 % BGP sample. These findings underscore the potential of Amura starch–bagasse composites as sustainable replacements for single-use plastics in packaging and lightweight applications. The obtained results imply that sugarcane bagasse, combined with amura starch, and glycerol can serve as an effective, biodegradable food packaging material, with potential of addressing impact of conventional plastics on environment.*

**Keywords:** Bio-composite, Biodegradable polymer, Sugarcane bagasse powder, Amura starch, Glycerol

## 1 INTRODUCTION

The global reliance on traditional fossil based plastics has triggered increasing concern over resource depletion, waste accumulation, and environmental persistence. Biopolymers derived from renewable sources promise to reduce these burdens by offering degradability, lowered carbon footprint, and circular economy potential [1, 2]. Among them, starch is particularly attractive due to its abundance, low cost, and inherent biodegradability [3, 4]. When processed with plasticizers into thermoplastic starch (TPS), starch can be melt processed similarly to conventional plastics—however, the

challenge remains that TPS typically exhibits inferior mechanical strength, thermal stability, and moisture resistance compared to petrol-based polymers [5, 6]. Recent reviews emphasize that to make TPS viable for broader applications, researchers must address formulation, processing, and reinforcement strategies in tandem [4, 7]. For example, integrating natural fillers, compatibilizers, and optimized plasticizers has shown promise in reinforcing starch-based systems [8, 9]. Moreover, another key direction is material systems grounded in regional feed-stocks and agric-waste valorization, which help align sustainability with local resource use [10, 11]. On the plasticizer front, glycerol remains the workhorse for starch-based bio-plastics due to its high solubility, low cost, and good plasticization efficiency [12, 13]. Nonetheless, high glycerol content can lead to elevated water uptake, lower thermal degradation onset, and faster retro gradation or ageing [14, 15]. Balancing glycerol level and compatibilization remains a critical lever for TPS systems [16]. In the realm of reinforcement, natural fibers have attracted increasing attention for enhancing biocomposite performance while maintaining renewable credentials. Among these, sugarcane bagasse—the fibrous residue remaining after cane-juice extraction—is abundant (estimates of global production approach hundreds of millions of tons annually) and well positioned for sustainable material substitution [17, 18]. Studies show that bagasse fiber content, particle size, and surface treatment strongly influence modulus, strength, water absorption, and thermal behaviour [19, 20]. Moreover, recent reviews highlight bagasse's potential across packaging, construction, and composite materials [21, 22]. Despite these advances, several practical gaps remain. First, many starches based composite studies use starch sources (e.g., corn, potato, cassava) rather than under-utilized starches with unique properties. Second, while bagasse fibers are being explored in polymeric matrices such as epoxy or PLA, their coupling with starch matrices (particularly plasticized TPS) remains relatively under-explored. Third, there is often limited systematic investigation linking starch source, plasticizer content (especially glycerol), fiber content/treatment, and a full set of property tradeoffs (mechanical, thermal, moisture, biodegradation) in one coherent framework. This leaves a gap between laboratory materials and viable application grade biocomposites [1, 13]. In this work, we develop biocomposites using a locally sourced starch from Tacca species (commonly referred to as 'Amura' starch) as the primary biopolymer matrix, glycerol as the plasticizer, and sugarcane bagasse powder as reinforcement. We systematically map the influence of glycerol level and bagasse content (with/without simple surface treatment) on processing (melt compounding or casting), structure (morphology, interfacial bonding), and properties (tensile, hardness, water uptake, and thermal stability). The novelty of this work lies in three aspects: (1) the use of Tacca/Amura starch a regionally available but under-studied biopolymer; (2) the pairing of this starch with untreated and treated sugarcane bagasse powder in a single formulation space; and (3) the explicit evaluation of glycerol-bagasse-starch interactions in a processing-structure-property context. This combination advances the field by bridging local resource valorization with full cycle composite design for sustainable materials.

## 2 MATERIALS AND METHODS

### 2.1 Materials

Amura starch was extracted from *Tacca leontopetaloides* tubers collected locally in Nigeria. Analytical-grade sulfuric acid ($H_2SO_4$), sodium hydroxide (NaOH), and ethanol (95%) were obtained from Local Source. Sugarcane bagasse was sourced from a local milling industry, thoroughly washed, and sun-dried prior to use. Glycerol (analytical grade, ≥ 99% purity) was used as a plasticizer. Distilled water was used throughout all experimental procedures.

### 2.2 Sample Preparation

#### *2.2.1 Preparation of Cellulose Nanocrystal (CNC) from Amura Starch*

Cellulose nanocrystals (CNCs) were produced from Amura starch following a controlled acid hydrolysis method adapted from [23, 24]. Briefly, 10 g of dried Amura starch powder was dispersed in 200 mL of 60 wt. % sulfuric acid solution and maintained at 45 °C under continuous stirring for 60 min. The reaction was quenched by adding an equal volume of cold distilled water, and the resulting suspension was centrifuged at 10 000 rpm for 10 min to remove excess acid. The sediment was dialyzed against distilled

water until neutral pH was achieved, followed by ultrasonication for 15 min to ensure homogeneous dispersion. The CNC suspension was then freeze-dried to obtain fine CNC powder for subsequent composite fabrication [7].

*2.2.2 Preparation of Sugarcane Bagasse Powder (BGP)*

Raw sugarcane bagasse was first washed with hot water to remove adhering sugars and impurities, then oven-dried at 60 °C for 24 h. The dried material was ground and sieved to obtain powder with a particle size below 150 µm. To remove lignin and hemicellulose, the powder was treated with 5 wt.% NaOH solution at 80 °C for 2 h, followed by thorough rinsing until neutral pH was reached [20]. The treated fibers were bleached using a mixture of 1.7 % sodium chlorite ($NaClO_2$) and acetic acid at 70 °C for 1 h, then filtered, washed, and oven-dried at 50 °C for 12 h. The resulting *sugarcane bagasse powder (BGP)* was stored in airtight containers before blending.

*2.2.3 Fabrication of Bio-Composite Samples*

Six formulations were prepared using constant starch and glycerol content but varying BGP loading: Sample A: Control (0% BGP + 5 mL glycerol), Sample B: 0.5% BGP + 5 mL glycerol, Sample C: 1.0% BGP + 5 mL glycerol, Sample D: 1.5 % BGP + 5 mL glycerol, Sample E: 2.0 % BGP + 5 mL glycerol, and Sample F: 2.5% BGP + 5 mL glycerol. The starch (10 g) was dispersed in 100 mL distilled water and heated to 75 °C with continuous stirring until gelatinization occurred. Glycerol and the required amount of BGP were gradually added, followed by mechanical stirring at 500 rpm for 30 min. The mixture was cast into Teflon molds and dried at 45 °C for 48 h to form uniform films. Dried samples were conditioned at 23 ± 2°C and 50 ± 5% relative humidity before characterization [25].

**2.3 Characterization Techniques**

*2.3.1 Fourier Transform Infrared (FTIR) Spectroscopy*

FTIR spectra were obtained using a Thermo Scientific Nicolet iS50 FTIR spectrometer operating in the range of 4000–400 $cm^{-1}$, at 4 $cm^{-1}$ resolution and 32 scans per sample. This analysis was used to identify functional groups and assess possible interactions between starch, glycerol, and bagasse [11].

*2.3.2 Universal Testing Machine (UTM) – Tensile and Hardness Tests*

Mechanical properties were determined using a Tensile strength testing machine (Model TM2101-T7, Capacity: 10 kN) according to ASTM D-638**.** Dog-bone-shaped specimens (100 × 20 × 3 mm) were tested at a crosshead speed of 10mm/min. Hardness was measured using a Vickers hardness test machine (Model MV1-PC, Capacity: 0.3 kgf) in accordance with ASTM E-384**,** with five indentations per specimen and averaged results reported [19].

*2.3.3 X-Ray Diffraction (XRD)*

Crystalline structure was analyzed using a Rigaku MiniFlex 600 X-ray diffractometer with Cu Kα radiation (λ = 1.5406 Å), operated at 40 kV and 30 mA. Scans were performed over a 2θ range of 5°–80° at 2° $min^{-1}$. The degree of crystallinity was determined using peak deconvolution methods [26].

*2.3.4 Thermogravimetric Analysis (TGA)*

Thermal stability of the composites was studied using a TA Instruments Q500 thermogravimetric analyzer under nitrogen flow (50 mL $min^{-1}$). Samples (≈ 10 mg) were heated from 25 °C to 600 °C at 10 °C $min^{-1}$. The derivative thermogravimetric (DTG) curves were used to identify decomposition stages [24].

*2.3.5 Moisture Absorption Test*

Moisture absorption was measured according to ASTM D570. Dried samples were weighed ($W_0$) and then immersed in distilled water at room temperature (25 °C) for 24 h. After removal, samples were gently wiped and reweighed ($W_1$). The percentage of moisture absorbed was calculated using:

$$Moisture\ absortion\ (\%) = \frac{W_1 - W_0}{W_0} \times 100 \quad (1)$$

Each test was repeated three times, and the average value was reported [5].

## 3 RESULTS AND DISCUSSION

### *3.1.1 Fourier Transform Infrared (FTIR) Analysis*

The FTIR spectra of Samples A–F (Figures 1 a–f) reveal the major functional groups associated with the *Tacca* (Amura) starch matrix, glycerol plasticizer, and sugarcane bagasse powder (BGP) reinforcement. In all spectra, a broad absorption band appeared around 3270 $cm^{-1}$, which corresponds to the stretching vibration of hydroxyl (O–H) groups from starch, cellulose, and glycerol molecules [23]. For the control sample (A, 0 % BGP), the O–H peak was relatively sharper and positioned at 3270.7 $cm^{-1}$ with a higher transmittance, indicating fewer hydrogen bonds. As the BGP content increased from 0.5 % to 2.5 %, the O–H band became broader and slightly shifted to lower wavenumbers (3268–3271 $cm^{-1}$), implying the formation of additional hydrogen bonds between the hydroxyl groups of the starch chains and the cellulose surfaces of bagasse fibers [20]. This shift confirms that physical intermolecular interactions occurred during composite formation, resulting in improved compatibility and interfacial adhesion within the bio-composite system. In the 2925–2850 $cm^{-1}$ region, weak absorption peaks were observed in all samples, which are attributed to C–H stretching of aliphatic $CH_2$ and $CH_3$ groups present in the polysaccharide backbone and glycerol molecules [25]. The intensity of these peaks slightly decreased at higher BGP loading levels, which can be explained by a reduction in free glycerol due to partial hydrogen bonding with fiber hydroxyl groups. This reduction suggests that glycerol molecules are effectively interacting with cellulose, thereby improving the homogeneity of the matrix. A medium-intensity peak appeared around 1635–1640 $cm^{-1}$ in all samples, representing O–H bending of absorbed water and minor C=O stretching vibrations from hemicellulose residues [19]. The intensity of this band decreased gradually from the control to higher BGP concentrations, indicating that the presence of bagasse powder reduced the amount of bound moisture within the composite [11]. This observation is consistent with the expected improvement in moisture resistance of the reinforced materials. The strong bands between 1150 and 1030 $cm^{-1}$ correspond to C–O–C and C–O stretching vibrations in the glycosidic linkages of starch and [26]. These peaks remained in all spectra, confirming that the main polysaccharide backbone structure was preserved throughout processing. However, a gradual increase in intensity and minor peak sharpening were observed at higher bagasse contents, especially in Samples D–F (1.5–2.5 % BGP). This behavior is associated with increased crystallinity and stronger hydrogen-bond networks due to the presence of cellulose nanostructures from bagasse fibers, which enhance matrix reinforcement. Additional peaks detected around 924, 851, and 758 $cm^{-1}$ are attributed to C–O–H bending and skeletal vibrations of glucose units within starch and cellulose [27]. The persistence of these peaks across all spectra confirms that no chemical degradation occurred during blending or drying. Instead, subtle intensity variations indicate differences in fiber dispersion and interfacial interaction across the formulations. Comparatively, Sample A (control) showed features typical of thermoplastic starch (TPS) films with limited hydrogen bonding and high hydroxyl availability. As small amounts of bagasse were introduced (Samples B and C, 0.5–1.0 %), the spectra showed broadening of the O–H band and a reduction in the water-bending peak, signifying better matrix–fiber interaction. Samples D and E (1.5–2.0 %) exhibited the most pronounced changes, with increased C–O–C and C–O intensities, suggesting optimal interfacial bonding and improved dispersion. At the highest loading (Sample F, 2.5 %), a slight decline in transmittance and intensity homogenization was noted, likely due to fiber agglomeration and reduced matrix continuity at excessive filler levels. Overall, the FTIR results confirm that no new covalent bonds were formed during processing; rather, hydrogen bonding is the dominant mechanism for the interaction between *Tacca* starch, glycerol, and sugarcane bagasse powder. Broadening of the O–H region and the changes in C–O–C intensity across the composite series, support successful integration of bagasse fibers within the starch matrix. These molecular interactions enhance mechanical cohesion and thermal stability, providing strong evidence that moderate fiber loading (1.0–1.5 %) yields optimal structural compatibility and composite performance [20, 23, 25].

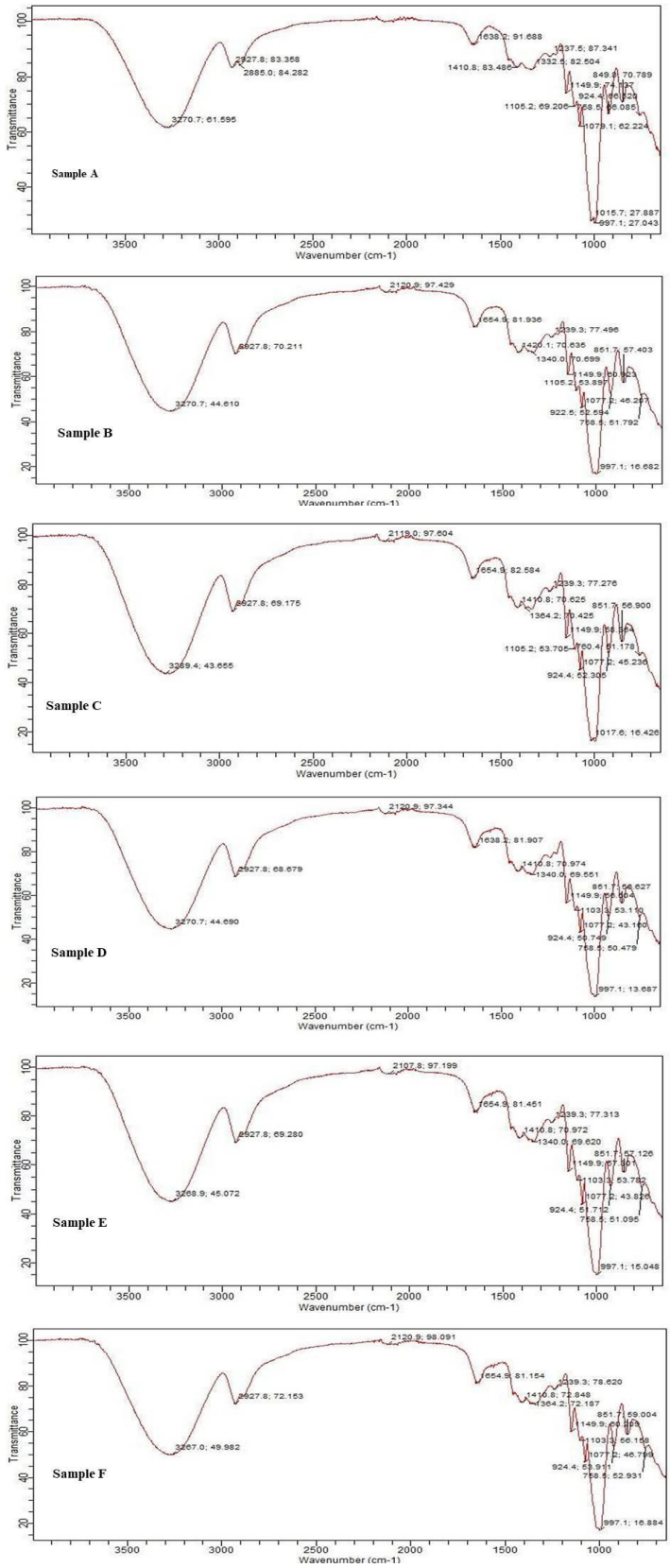


Figure 1. FTIR spectra of bio-composite samples A–F (0–2.5 % BGP)

### 3.2 Universal Testing Machine (UTM) analysis

#### *3.2.1 Tensile Stress–Strain Behavior*

Figure 2 presents the tensile strength versus elongation curves for the six bio-composite samples (A–F) containing varying loadings of sugarcane bagasse powder (BGP) in the glycerol-plasticized *Tacca* starch matrix. The stress–strain profile of each sample reveals the effect of fiber reinforcement on the deformation and fracture behavior of the composites. The control sample (A), composed solely of Amura starch and glycerol, exhibited the lowest tensile strength and shortest elongation, confirming the inherent brittleness and low stress-bearing capacity of neat thermoplastic starch (TPS). Its early fracture and steep curve indicate weak molecular entanglement and limited chain interaction, which are typical characteristics of unreinforced starch films [23]. With the introduction of 0.5 %, 1.0% and 1.5 % bagasse powder (Samples B, C, and D), both the maximum stress and the area under the curve increased substantially. This improvement signifies that the dispersed cellulose fibers provided additional load-bearing paths and enhanced hydrogen bonding between the hydroxyl groups of starch and cellulose [20]. The resulting network restricted chain slippage, improving stiffness and tensile resistance. At 2 % BGP (Sample E), the composite achieved the highest peak tensile strength (~2.5 MPa) and maintained moderate elongation, indicating optimal stress transfer efficiency and strong interfacial adhesion between the matrix and reinforcement [19]. This optimum performance is consistent with the FTIR results, where broader O–H stretching bands confirmed stronger hydrogen-bond interactions. Beyond the 2.0 % reinforcement threshold, the mechanical response began to deteriorate. Samples F (2.5 % BGP) displayed slightly lower tensile strength and reduced strain-at-break values. The curve shapes became less uniform, suggesting the presence of [25]. Excess cellulose powder likely led to weak interfacial regions and void formation, causing premature failure under applied stress. Nevertheless, the reinforced composites still demonstrated higher tensile performance than the unfilled starch film, confirming that even moderate filler levels impart structural benefits. Overall, the progression of these curves clearly demonstrates the transition of the material from a ductile starch matrix to a semi-rigid, fiber-reinforced bio-composite. The enhanced mechanical behavior up to 2.0 % BGP is attributed to a balance between fiber dispersion and matrix cohesion, while further addition introduces interfacial discontinuities that negate the reinforcement effect [7, 11]. These results confirm that an intermediate loading of sugarcane bagasse fibers offers an optimal combination of strength and flexibility, suitable for applications such as biodegradable packaging and light structural materials.

#### *3.2.2 Hardness Behavior*

Figure 3, the surface hardness of the *Tacca* starch–sugarcane bagasse bio-composites was evaluated using the Vickers hardness test (Model MV1-PC, capacity 0.3 kgf) in accordance with **ASTM E-384.** The average hardness values obtained for the six samples are as follows: control (3.8 HV), 0.5 % BGP (5.5 HV), 1.0 % BGP (4.2 HV), 1.5 % BGP (6.2 HV), 2.0 % BGP (6.7 HV), and 2.5 % BGP (8.5 HV). These results indicate a general trend of increasing hardness with higher fiber loading, except for a minor dip at 1.0 % BGP, which can be attributed to localized non-uniform dispersion of bagasse particles within the matrix. For the control sample, the relatively low hardness value (3.8 HV) reflects the soft and flexible nature of pure glycerol-plasticized starch. The plasticizer disrupts intermolecular hydrogen bonds among starch chains, thereby reducing rigidity and increasing free-volume mobility within the polymer structure [23]. Upon the incorporation of 0.5 % BGP, the hardness rose sharply to 5.5 HV due to the stiffening effect imparted by the cellulose-rich bagasse powder. The presence of these lignocellulosic fillers introduces additional hydrogen bonding sites that restrict polymer chain movement, resulting in a denser microstructure [20]. Although the 1.0 % BGP composite exhibited a slight reduction (4.2 HV), this may have arisen from small clusters of undispersed fibers acting as micro-void sites, which reduce uniform stress transfer at the indentation zone. However, further increases in fiber loading restored and enhanced the hardness significantly. At 1.5 % BGP and 2.0 % BGP, the hardness improved to 6.2 HV and 6.7 HV, respectively, demonstrating effective reinforcement and stronger starch–fiber interfacial adhesion. The highest hardness

value (8.5 HV) was observed at 2.5 % BGP, indicating a more compact structure with higher surface resistance to deformation [19, 25]. This progressive improvement in hardness with increased filler content aligns with the enhanced stiffness observed in the tensile test. The incorporation of sugarcane bagasse fibers promotes efficient load sharing and minimizes localized deformation under applied force. The trend also suggests that the cellulose component of the bagasse contributes to micro-crystalline reinforcement, thereby increasing the packing density of the bio-composite [27]. However, at excessive filler levels beyond the optimum (2.5 %), the risk of agglomeration could potentially offset these gains by creating brittle micro-zones, as indicated by the sharp hardness rise without a proportional improvement in elongation. Overall, the hardness behavior confirms that the mechanical rigidity of the *Tacca* starch composites can be effectively tuned through controlled incorporation of bagasse powder. The strong interfacial hydrogen bonding between the starch matrix and the cellulose fibers enhances surface durability and indentation resistance [7, 11].

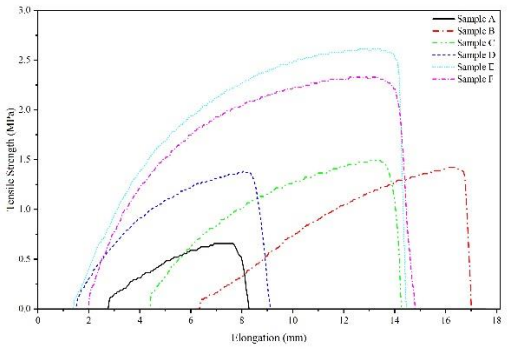


Figure 2. Presents the tensile strength versus elongation curves for the six bio-composite samples (A–F)

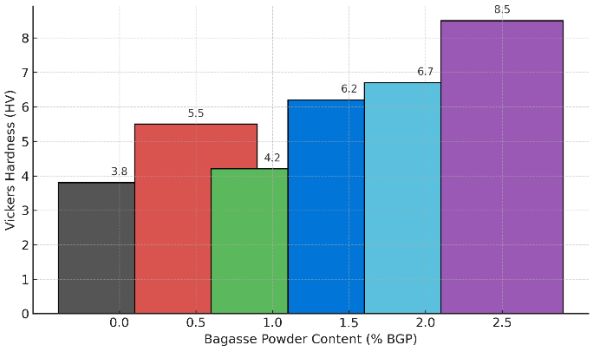


Figure 3. Variation of Vickers hardness (HV) with bagasse powder content (% BGP) for the six bio-composite samples (A–F)

### 3.3 X-Ray Diffraction (XRD) Analysis

The X-ray diffraction (XRD) patterns of the *Tacca* starch–sugarcane bagasse bio-composites at 0.5% and 2.0% bagasse powder (BGP) loadings are shown in Figures 4(a) and 3.4(b), respectively. These patterns were analyzed to determine the crystalline phases and structural changes induced by the incorporation of lignocellulosic fibers into the starch matrix. Both composites displayed broad peaks in the range of $2\theta = 10°–25°$, which is characteristic of the semicrystalline nature of starch-based biopolymers The broad halo centered near $2\theta \approx 16°–18°$ corresponds to the overlapping reflections of the (110) and (200) planes of A-type starch crystallites, while the diffuse background indicates an amorphous phase resulting from plasticization with glycerol [20]. For the 0.5% BGP sample, the diffractogram revealed a prominent broad peak at around $2\theta \approx 17°$, suggesting the retention of the starch crystalline domains with moderate ordering. Minor reflections corresponding to silicon oxide ($SiO_2$), aluminum phosphate ($AlPO_4$), and trace minerals such as hanksite ($Na_{22}K(SO_4)_9(CO_3)_2Cl$) and anhydrite ($CaSO_4$) were also identified. The presence

of these inorganic components, originating from bagasse ash and residual minerals, contributes to the composite's enhanced structural rigidity [19]. The identified phases such as refikite and chaoite indicate possible reorganization of polysaccharide chains and microcrystalline impurities introduced during acid hydrolysis of starch. The relatively broad peaks and absence of sharp crystalline reflections confirm that the material remains predominantly amorphous, a typical feature of glycerol-plasticized starch systems [7]. At 2.0% BGP loading, a noticeable change in the XRD pattern was observed. The main amorphous peak at 17° became less intense and more diffuse, indicating a further disruption of the starch crystalline regions due to the higher incorporation of cellulose fibers. New minor crystalline peaks appeared at $2\theta \approx 22°–25°$, which can be attributed to the (002) plane of cellulose I and mineral constituents such as silicon oxide, aluminum phosphate, and simonellite ($C_{19}H_{24}$), confirming partial crystallization of the lignocellulosic reinforcement [27]. The reduction in starch crystallinity suggests that fiber incorporation led to partial restriction of chain mobility, hindering the recrystallization of amylose and amylopectin during drying. This phenomenon results in a more heterogeneous microstructure comprising amorphous starch domains and embedded cellulose crystallites, consistent with the improved mechanical hardness observed in Section 3.2.2. Comparatively, the 0.5% BGP composite exhibited a more defined starch-based crystalline peak, while the 2.0% BGP sample displayed a broader amorphous halo with multiple minor crystalline reflections. This evolution confirms that the addition of bagasse fibers induces a starch-to-cellulose phase transition, where hydrogen bonding between hydroxyl groups in starch and cellulose disrupts the regular packing of starch granules while promoting localized ordering within the cellulose microdomains [11, 26]. Such hybrid microstructures are desirable for enhancing dimensional stability and mechanical strength while maintaining sufficient flexibility for bio-composite applications. In summary, the XRD results demonstrate that the *Tacca* starch/bagasse composites consist of a semicrystalline matrix, where starch contributes the amorphous character, and cellulose fibers introduce crystalline reinforcement. The partial crystallization and mineral inclusions enhance the interfacial compatibility between organic and inorganic phases, confirming the structural stability of the developed bio-composites.

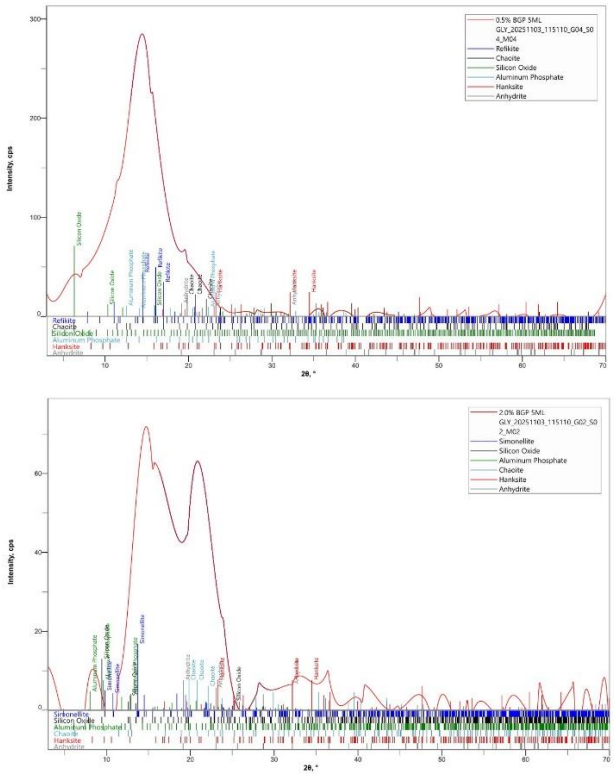


Figure 4. X-ray diffraction (XRD) patterns of *Tacca* starch–sugarcane bagasse composites

### 3.4 Thermogravimetric Analysis (TGA)

The thermal stability of the *Tacca* starch–sugarcane bagasse bio-composites was evaluated using thermogravimetric analysis (TGA) under a nitrogen atmosphere, and the resulting thermograms for Samples B–E are presented in Figure 5. The curves display the relationship between temperature and percentage weight loss, which provides insight into the degradation pattern of the composites and the influence of fiber loading on their thermal resistance. In general, all samples exhibited three main stages of weight loss, corresponding to (i) moisture and volatile evaporation, (ii) polymer decomposition, and (iii) carbonaceous residue formation [23]. The first stage occurred between 30–150 °C, with a minor mass loss of approximately 5–10 %, attributed to the evaporation of adsorbed water and glycerol from the hydrophilic starch–cellulose matrix [20]. The second and most significant stage took place within the 250–380 °C range, corresponding to the thermal decomposition of starch chains, cellulose, and hemicellulose components in both the matrix and bagasse reinforcement [25]. In this region, a steep decline in mass indicates depolymerization and the breakdown of glycosidic bonds. The third stage, extending beyond 400 °C, represents the slow degradation of residual char and the oxidation of lignin and other aromatic fragments [19]. Among the composites, the control-type formulations (lower BGP loadings: Samples B and C) showed slightly earlier onset of degradation, suggesting lower heat tolerance. In contrast, the samples containing higher fiber content (Samples D and E) exhibited improved thermal stability, evidenced by a delayed degradation onset and a higher residual weight above 500 °C. The 2.0 % BGP composite (Sample E) showed the highest char yield, retaining nearly 20 % of its mass at 600–700 °C, compared with less than 10 % for lower fiber loadings. This enhanced stability can be attributed to the formation of a thermally stable carbonaceous structure provided by the lignocellulosic bagasse and the mineral-rich ash constituents detected in XRD analysis (silicon oxide, aluminum phosphate, and calcium sulfate), which act as heat barriers and char promoters [11, 26]. The incorporation of cellulose fibers increased crosslinking density and restricted the mobility of starch molecular chains, thereby improving the composite's ability to withstand thermal decomposition. Furthermore, the interaction between starch hydroxyls and cellulose through hydrogen bonding likely hindered the volatilization of small molecular fragments, contributing to the observed delay in weight loss [27]. The TGA data therefore confirm that the inclusion of sugarcane bagasse powder enhances the overall thermal resistance of the *Tacca* starch matrix. The improved thermal behavior at moderate fiber loadings supports the material's suitability for thermoforming and packaging applications where moderate heat resistance is required.

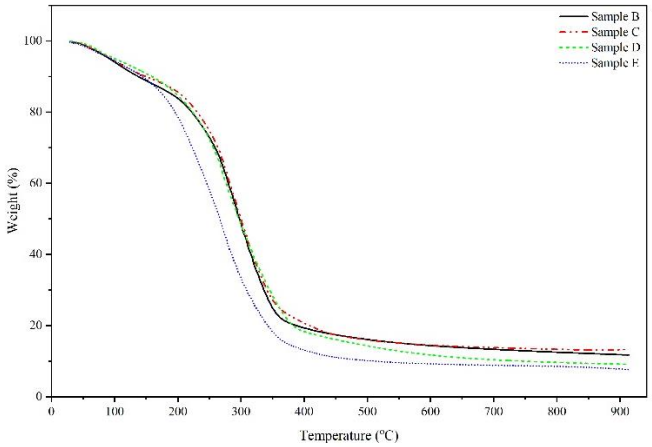


Figure 5. Thermogravimetric analysis (TGA) curves of *Tacca* starch–sugarcane bagasse bio-composites with 5 mL glycerol at varying BGP contents (0.5 %, 1.0 %, 1.5 %, and 2.0 %)

The DTG profiles (Figure 6) highlight the temperature regions where mass loss is most rapid and make the differences among formulations explicit. All samples show a small, shallow feature below 100–

120 °C, attributed to the evaporation of physically bound moisture and traces of free glycerol; the low magnitude confirms minimal volatile content after conditioning. The dominant single peak for each sample lies in the ~270–330 °C window and corresponds to the concerted depolymerization of glycerol-plasticized starch together with cellulose/hemicellulose in the bagasse filler. The temperature of maximum decomposition rate, $T_{max}$, and the peak depth (absolute derivative) are the best comparators of thermal robustness. Samples B and D (0.5 % and 1.5 % BGP) display very similar $T_{max}$ values around ~300–310 °C with moderately deep peaks, indicating comparable primary degradation kinetics and suggesting good matrix continuity with effective—but not catalytic—filler interaction. Sample C (1.0 % BGP) exhibits the deepest peak (≈ −5 % · °C⁻¹) centered close to ~305–315 °C, implying the highest instantaneous mass-loss rate among the series and thus a slightly less thermally robust network at that loading. In contrast, Sample E (2.0 % BGP) shifts its main DTG peak toward lower temperatures (~280–295 °C) and shows an earlier, broader onset. This leftward shift and broadened profile indicate earlier activation of degradation pathways, consistent with the lower residual mass observed in the corresponding TGA curve and attributable to (i) reduced matrix continuity at higher filler volume fraction and/or (ii) catalytic effects of mineral ash associated with bagasse (e.g., siliceous or phosphate species) that can promote dehydration and scission reactions. Above ~400 °C, DTG signals approach zero for all samples, reflecting the slow transformation of carbonaceous char and thermally persistent fragments. Minor end-effects near ~850–900 °C are small and sample-to-sample variations are within typical instrumental baseline noise for low-mass residues. Taken together the DTG analysis points to an optimal fiber loading near 1.5 % (Sample D) for maintaining a relatively high $T_{max}$ with a restrained mass-loss rate, whereas excess filler (2.0%) accelerates degradation and reduces thermal endurance. These kinetic observations are consistent with the mechanical trends (stiffening to an optimum, then deterioration) and with the XRD evidence of increasing heterogeneity and mineral contributions at higher BGP content [3, 29].

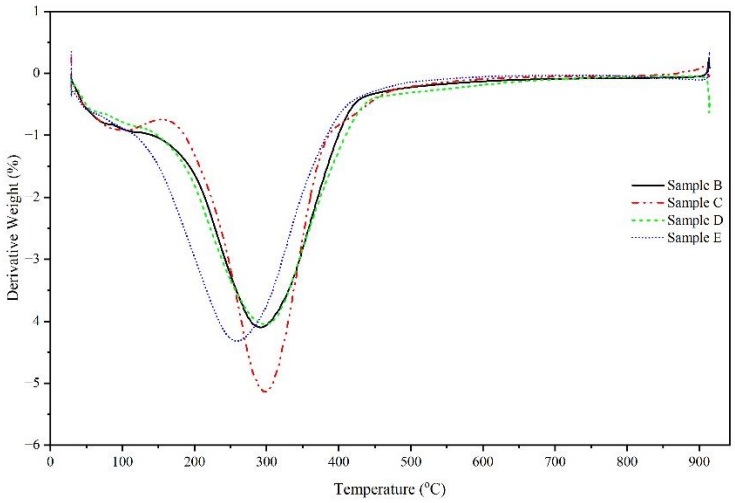


Figure 6. Derivative thermogravimetric (DTG) curves of glycerol-plasticized *Tacca* starch composites at different bagasse powder (BGP) loadings (Samples B–E)

### 3.5 Moisture Absorption Analysis

The moisture absorption characteristics of the *Tacca* starch–sugarcane bagasse composites were investigated to evaluate their hydrophilic nature and the influence of bagasse content on water uptake. The measured values summarized in Table 1, show that the moisture absorption (%) of the samples ranged from 11.85 % to 16.76 %, depending on the bagasse powder (BGP) content. The control sample containing 5 mL glycerol and no BGP exhibited a moisture absorption value of 14.31 %, which reflects the intrinsic hydrophilicity of the starch–glycerol matrix [23]. Glycerol, being a low molecular weight plasticizer with multiple hydroxyl groups, tends to increase water affinity by creating free volume and hydrogen-bonding

sites within the polymer structure [7]. With the introduction of 0.5 % and 1.0 % bagasse powder, the water uptake increased slightly to 15.36 % and 16.17 %, respectively. This behavior can be attributed to the hydroxyl-rich cellulose and hemicellulose components of the bagasse fibers, which also possess strong affinity for moisture [20]. The presence of these fibers at low concentrations enhances capillary sorption and creates more hydrophilic microregions on the composite surface, promoting water diffusion (Ismail et al., 2024). However, a distinct decrease in moisture absorption was observed at 1.5 % and 2.0 % BGP (12.30 % and 11.85 %, respectively). This reduction is associated with improved interfacial bonding between starch and cellulose, which limits the availability of free hydroxyl groups for water interaction. The formation of extensive hydrogen bonds between starch chains and cellulose fibrils reduces water penetrability and suppresses swelling of the polymer matrix [27]. At the highest filler loading of 2.5 % BGP, the moisture absorption again increased to 16.76 %, indicating that excessive fiber addition introduced interfacial voids and aggregation, allowing water to diffuse more easily through micro-capillaries [25]. This trend reflects a critical balance between fiber dispersion and interfacial saturation: moderate reinforcement (1.5–2.0 %) promotes compact packing and reduced porosity, while excessive filler loading compromises homogeneity and increases hydrophilic surface area. Similar patterns have been reported in starch–cellulose systems, where optimum filler content yields the lowest water absorption due to strong matrix–filler adhesion [11]. The results demonstrate that fiber incorporation significantly influences the hydrophilicity and dimensional stability of the bio-composites. The reduction in water uptake at intermediate bagasse levels corresponds well with the enhanced mechanical strength and thermal stability observed in the preceding sections. These correlations confirm that improved starch–cellulose interaction minimizes water sensitivity by stabilizing the polymer network, thus making the composites more suitable for semi-dry packaging or biodegradable film applications where moderate moisture resistance is desirable [26].

Table 1. Moisture absorption of *Tacca* starch–sugarcane bagasse bio-composites with 5 mL glycerol at varying BGP contents.

| S/N | Sample | Initial Weight (g) | Final Weight (g) | Moisture Absorption (%) |
|---|---|---|---|---|
| 1 | Control (5ml Glycerol) | 0.601 | 0.687 | 14.309 |
| 2 | 0.5% BGP 5ml Glycerol | 0.690 | 0.796 | 15.362 |
| 3 | 1.0% BGP 5ml Glycerol | 0.711 | 0.826 | 16.174 |
| 4 | 1.5% BGP 5ml Glycerol | 0.919 | 1.032 | 12.296 |
| 5 | 2.0% BGP 5ml Glycerol | 0.987 | 1.104 | 11.854 |
| 6 | 2.5% BGP 5ml Glycerol | 0.692 | 0.808 | 16.763 |

### 3.6 Environmental Relevance and Sustainability Perspective

The development of these *Tacca* starch–sugarcane bagasse bio-composites represents a critical advancement in sustainable material design, directly addressing the growing concerns over plastic pollution and agricultural waste management. Conventional petroleum-based plastics persist in the environment for centuries, releasing toxic compounds during degradation, whereas the present bio-composite system is entirely derived from renewable and biodegradable resources [7]. The use of *Tacca leontopetaloides* starch as a base polymer offers a sustainable alternative to synthetic resins while promoting the utilization of an underexplored local crop, contributing to rural economic value chains and biodiversity conservation [23]. Similarly, sugarcane bagasse—an abundant by-product of the sugar industry—is often disposed of by open burning, which releases greenhouse gases and particulates into the atmosphere. By converting this residue into a functional reinforcement for biodegradable composites, the present study supports the **circular bio-economy** concept, transforming agro-waste into high-value products [20]. Moreover, the fabrication route used in this study relies on low-energy processing **and** non-toxic ingredients**,** aligning with green chemistry principles and minimizing the carbon footprint associated with production. The resulting composites exhibit mechanical strength and moisture resistance comparable to commercial biodegradable films, indicating their potential substitution for short-life packaging, disposable utensils, and agricultural mulch films [25]. Hence,

this research not only demonstrates a viable material innovation but also contributes to broader sustainability goals—reducing reliance on fossil resources, preventing biomass waste mismanagement, and promoting locally adaptable, eco-friendly materials for a cleaner environment [11, 19].

## 4 CONCLUSIONS

This research successfully developed a series of biodegradable bio-composites from *Tacca leontopetaloides* (Amura) starch reinforced with sugarcane bagasse powder and plasticized with glycerol. The integration of lignocellulosic bagasse into the starch matrix markedly enhanced interfacial bonding, mechanical integrity, and thermal resilience. The optimal composite containing 1.5 % BGP exhibited the best synergy of tensile strength, hardness, and stability, confirming efficient stress transfer and matrix–fiber compatibility. Moderate fiber loading also minimized water uptake, demonstrating improved dimensional stability and resistance to moisture. These findings establish *Tacca* starch as a promising renewable polymer source and illustrate that agro-waste bagasse can serve as a functional reinforcement to create low-cost, eco-friendly materials. Beyond the laboratory, this combination represents a sustainable path toward replacing conventional plastics in packaging, disposable ware, and light structural components. Future work should extend to biodegradation kinetics, surface modification of fibers, and compatibilizer optimization to further refine performance for commercial adoption.

## ACKNOWLEDGEMENT

The authors wish to acknowledge the NAUB directorate for research and innovation, for the award of TETFUND institution-based research (IBR) project 2024.

## REFERENCES

1. Kouka, S., Benmoussa, A. and Saffana, K. (2025). Global trends and circularity in bio-based polymer production. *Renewable and Sustainable Energy Reviews*, vol. 189, pp. 114082.
2. Zhou, Y., Huang, C. and Zhang, Q. (2024). Sustainable biopolymer production and circular-economy strategies: A global review. *Sustainable Materials and Technologies*, vol. 39, pp. 00784.
3. Mohammed, S., Noor, N. and Bahri, S. (2022). Plasticizers in thermoplastic starch films: Structure-property relationships. *Polymers*, vol. 14, no. 11, pp. 21-52.
4. Sobeih, A.E., Abdelrahman, M. and Tawfik, M. (2025). Starch-based bioplastics and biocomposites: State of the art and future perspectives. *Materials*, vol. 18, no. 5, pp. 20-93.
5. Fernández, C.L., Martínez, J.D. and Pérez, R.A. (2025). Optimization of glycerol–honey plasticized cassava starch films for biodegradable packaging. *International Journal of Food Science & Technology*, vol. 60, no. 1, pp. 50-62.
6. Wang, L., Liu, Z. and Li, H. (2024). Mechanical and thermal performance of thermoplastic starch films: Limitations and optimization routes. *Journal of Applied Polymer Science*, vol. 141, no. 17, pp. 54462.
7. Huang, W., Zhao, F. and Wu, Y. (2025). Bioplastics from renewable resources: A review on starch, PLA, and PHA systems. *Science of the Total Environment*, vol. 9, no. 42, pp. 172456.
8. Gurunathan, T., Rao, M. and Ahamed, R. (2025). Starch-based bioplastics: Progress, limitations, and recent developments. *Scientific Reports*, vol. 15, pp. 4733.
9. Assala, T., Toufik, C., Soufiane, B., Meyada, K., Fares, M.L.R., Elyes, K., Şükran, A.U., Furkan, T.S., Maria, D. and Luca, R. (2025). Cassava Starch–Onion Peel Powder Biocomposite Films: Functional, Mechanical, and Barrier Properties for Biodegradable Packaging. *Polymers*, vol. 17, no. 19, pp. 26-90.
10. Withana, N., Perera, D. and Fernando, A. (2025). Biodegradation of starch-based bioplastics in natural soils: A comparative study. Environmental Science: *Processes and Impacts*, vol. 27, no. 3, pp. 515-529.

11. Gadaleta, A., Cavallaro, G. and Lazzara, G. (2025). Environmental biodegradation behavior of starch-based bioplastics: Current understanding and challenges. *Polymers,* vol. 17, no. 3, pp. 651.
12. Michele, K.LT., Fernanda, F.C., Pedro, R.K., Daiane, H., Willian, Y.T., Arthur, S.P.J., Carolina, W.G., Ernandes, T.T.N. and Rafael, M.E. (2023). Azospirillum brasilense AbV5/6 encapsulation in dual-cross-linked beads based on cationic starch Carbohydrate *Polymers*, vol. 306, pp. 120631.
13. Patidar, R. and Goel, S. (2024). Green compatibilization and plasticization of starch-based composites: A critical review. *International Journal of Biological Macromolecules*, vol. 258, pp. 128-746.
14. He, L., Zhang, J. and Zhang, H. (2024). Morphological and mechanical characteristics of PBAT/thermoplastic starch blends with glycerol plasticization. *Polymers,* vol. 16, no. 5, pp. 905.
15. Syafri, E., Asrofi, M. and Sapuan, S.M. (2023). Plasticizer type and concentration effects on the properties of thermoplastic starch composites. *Polymers,* vol. 15, no. 8, pp. 18-21.
16. Hong-Ju, H., Guanglei, L., Mohammed, O. and Xingqi, O. (2025). Advances in Starch Digestibility: Insights from Multi-Scale Structure and Physical Modification, *Food and Bioprocess Technology*, vol. 18, no. 10, pp. 8223-8259.
17. Alessio, F., Fabrizio, C. and David, P. (2022). Structuring Circular Objectives and Design Strategies for the Circular Economy: A Multi-Hierarchical Theoretical Framework. *Sustainability*, vol. 14, no. 15, pp. 92-98.
18. Zafeer, M.A., Singh, A. and Kumar, A. (2023). Mechanical characterization and prospects of sugarcane bagasse fiber composites. *Journal of Natural Fibers,* vol. 20, no. 15, pp. 12322-12339.
19. Ismail, A., Rahman, M.N. and Saad, M. (2024). Surface modification of sugarcane bagasse fiber and its impact on mechanical and thermal properties of composites. *Polymers,* vol. 16, no. 7, pp. 12-34.
20. Chougala, A.D., Gowda, A.C., Santhosh, N. and Muhammad, I.A. (2024). Effect of Chemical Treatments on Mechanical Properties of Sugarcane Bagasse (Gramineae Saccharum Officinarum L) Fiber Based Biocomposites: A Review. *Journal of Natural Fibers*, vol. 22, no. 2, pp. 144-158.
21. Mawardi, M., Wicaksono, A.P. and Raharjo, S. (2025). Engineered bioboards from sugarcane bagasse and coir fibers using thermoplastic starch PVAc matrix. *Journal of the Korean Wood Science and Technology*, vol. 53, no. 4, pp. 571-584.
22. Stroescu, M., Stoica-Guzun, A. and Jinga, S. (2024). Circular use of agricultural residues in biopolymer production. Resources, *Conservation and Recycling*, vol. 208, pp. 106-916.
23. Carlos, C.A., Diner, M.M., Fernández-Jeri, A.B., Robert, J.C., Roberto, C.M.Z., Alex, J.V., Ilse, S.C.C., Guimarães da Silva, J., Nayara, M.P.A., Efraín, M.C.A. and Balcázar-Zumaeta, C. R. (2025). Polymers Derived from Agro-Industrial Waste in the Development of Bioactive Films in Food. *Polymers*, vol. 17, no. 3, pp. 4-08.
24. Pooja, M., Kumar, R. and Singh, D. (2025). Thermoplastic starch elastomers crosslinked with citric acid for improved flexibility. *International Journal of Biological Macromolecules*, vol. 266, pp. 133-495.
25. Mahmud, R.S., Hussin, M.W. and Ismail, H. (2025). Mechanical performance of chemically modified starch–bagasse composites. *Case Studies in Construction Materials*, vol. 23, pp. 19-83.
26. Yonata, M.H., Irawan, H. and Sari, P. (2025). Formation of resistant starch type III from Tacca leontopetaloides under acid–heat processing. *Food Chemistry*, vol. 434, pp. 137033.
27. Teo, E.Y., Hamzah, M.H. and Lau, Y.H. (2023). Sugarcane bagasse nanocellulose: Extraction, surface modification and application in composites. *Gels,* vol. 9, no. 5, pp. 377.
28. Osman, T., Rahman, M. and Harun, N. (2025). Comparative study on alkaline treatments of natural fibers: Effect on surface morphology and thermal properties. *Polymers*, vol. 17, no. 5, pp. 7-65.